CREATING AN OSTEOCHONDRAL BIOREACTOR FOR THE SCREENING OF TREATMENTS FOR OSTEOARTHRITIS

Derek A. Nichols[1], Inderbir S. Sondh[2], Paolo Zunino[1,4], Riccardo Gottardi[3,5]

[1]*Department of Mechanical Engineering and Materials Science,* [2]*Department of Bioengineering,* [3]*Department of Orthopedic Surgery, University of Pittsburgh;* [4]*Department of Mathematics, Politecnico di Milano, Italy;* [5]*Ri.MED Foundation, Palermo, Italy*

Abstract

Bioreactors are systems that can be used to monitor the response of tissues and cells to candidate drugs. Building on the experience developed in the creation of an osteochondral bioreactor at the University of Pittsburgh, we designed a new system which will allow constant optical access to the cells throughout testing unlike our previous model which limited observations to end-point testing. This new design was optimized in order to achieve the maximum possible fluid transport through the central chamber which corresponds to the maximum possible drug exposure. This was achieved by minimizing the channel diameter while maximizing the step height, outer ring diameter, pore diameter, and number of pores. A model with maximized drug exposure was then created and tested in a laboratory setting.

Keywords: Bioreactor, osteoarthritis, computational fluid dynamics, ANSYS CFX

Abbreviations: Osteoarthritis (OA), osteochondral (OC)

1 Introduction

Osteoarthritis (OA) is characterized by the breakdown of the cartilage lining the ends of long bones [1]. When studying the mechanism of OA progression to identify possible therapies, it is crucial to consider both bone and cartilage simultaneously as there is growing evidence suggesting interplay between them [1, 2].

Currently, there is no pharmacological treatment to arrest or cure cartilage degeneration during OA [1]. In order to screen drug candidates to identify potential treatments for OA while excluding potentially harmful compounds, it would be beneficial to possess systems of medium to high throughput screening that recapitulate the three-dimensional organization of cells within a tissue and that are thus more biosimilar to human physiology than cells in a dish [3]. Such systems would be used prior or in parallel to animal testing to decrease the need of animal use and increase the safety profile of the screen candidate drugs [4]. Appropriate bioreactors for this purpose are then necessary, i.e., apparatuses in which to place and maintain native tissues or cells in a 3D scaffold environment whose response to a candidate drug can be monitored. Some of our recent work has resulted in one such device for the study of osteochondral (OC) tissues or engineered constructs, that is, a physiological unit composed of cartilage and its subchondral bone [1, 5, 6]. This osteochondral system bioreactor is unique as it can be used to generate engineered OC constructs comparable in size to native tissues, and it can also be used to culture native tissue over several weeks (unpublished results). The current bioreactor system (fig. 1) which consists of a 3D printed part filled with an OC construct which is hooked up to a pump containing drugs and other nutrients, relies heavily on end-point testing, i.e., assessment of the effects of treatment by destructive tests such as PCR and histology, since it does not allow for direct optical access to the cells. Having such an optical access would allow the periodic, non-destructive monitoring of cell behavior, using, for instance, fluorescently labeled cells or cells transduced with gene reporters, which keep the cells and construct intact for future observations and tests.

FIGURE 1

To address this issue, the aim of this project was to design and optimize a new bioreactor system that would allow optical access to cells within 3D engineered constructs. We have achieved this objective by optimizing via finite element modelling a design that meets the required design parameters (small unit to host constructs to allow complete volumetric imaging, sufficient flow through the constructs to allow nutrients and waste exchange, size and fluidic channels compatible with a 96-well plate format), followed by 3D printing of the bioreactor and its testing.

2 Methods

2.1 Finite element modelling

Models of the flow path were created using the CAD software SolidWorks (Waltham, MA) and tested using the finite element analysis software ANSYS Fluid Flow (CFX) (Canonsburg, PA). A volume flow rate of 1 mL/day was imposed at the inlet, and the outlet was open to the environment. The chamber hosting the cells (central chamber) was considered as filled with photocrosslinked methacrylated gelatin (GelMA), a hydrogel with a permeability of $1*10^{-16}$ m^2 and a porosity of 0.8 [7]. Velocities through the central chamber were measured in CFX Post, the data resulting from the ANSYS simulation, and plotted against each specific design change in the bioreactor schematics to determine any relationships between design features and central velocity. Each model was assessed based on the velocity of the fluid through the middle of the central chamber as this is a fair representation of drug exposure throughout.

2.2 3D printing

The bioreactor was printed by stereolithography (SLA) using a 3Dsystems Viper si2 (Rock Hill, SC) printer and Somos WaterShed XC 11122 (Elgin, IL) resin. The resolution of the printer is 50 μm and the smallest possible void able to be printed is 0.60 mm [8, 9].

2.3 Fluidic validation

Once the bioreactor was printed and assembled, the central chamber was filled with GelMA. The inlet was then hooked up to a syringe filled with water which was in turn hooked up to a Kiyatec FC230 (Greenville, SC) pump which forced the water through the bioreactor at a rate of 1 mL/day [10]. Food dye was added to the water in order to better observe the flow through the central chamber. Pictures were then taken in 15 minute intervals in order to observe the flow of the fluid through the bioreactor.

3 Results

3.1 Bioreactor design

In order to allow for optical access to the cells, the thickness of the cell construct could not exceed 1 mm in height as this is the focal range of a standard microscope. The main block of the bioreactor (fig. 2a) which houses the GelMA in the central chamber and contains the path for the fluidics (fig. 2b) is assembled with the addition of other components (fig. 3).

FIGURE 2

FIGURE 3

Cells are hosted in the central chamber within a scaffold with low permeability, resulting in a relatively low amount of drug exposure since most of the fluid will travel through the surrounding channel [1]. The specific goal for this research was to define the optimal fluidic design of an

individual bioreactor chamber, such as the one seen in Figure 2b, that allows complete permeation of the engineered constructs with nutrients and other factors. The medium flow can be controlled by changing the geometric properties of the flow channels to control local pressure differences, and the effectiveness of the model can be quantified by measuring the velocity of the fluid through the central chamber. In fact, since the volume flow rate at the inlet is fixed, the higher the velocity through the central chamber, the greater the amount of total mass flow, and more mass flow equates to higher drug and nutrient exposure for the cells over time.

3.2 Design optimization

Optimization of the bioreactor can be achieved by altering the dimensions of the features found in Figure 4 as these dimensions are what control the flow through the model.

FIGURE 4

One dimensions can be increased in 0.05 mm increments while all other dimensions remain constant. The fluid velocity in the central chamber can then be plotted against the dimension of the design parameter of interest. Doing so for all dimensions results in the plots show in Figure 5.

FIGURE 5

Fluid velocity is linearly dependent on the step height, outer ring diameter, pore diameter, and number of pores whereas the correlation with the channel diameter is logarithmic and becomes linear when both variables are plotted on a log scale. Once parameter constraints are defined, it is possible to identify the maximum flux through the central chamber hosting the engineered constructs by simply using these linear relationships for each design feature.

Using these relationships, an optimized bioreactor was created, and the ANSYS results could be compared to a simple circular ring model in order to determine how the design was improved by optimizing the features from Figure 4. The results from the simulation are seen in Figure 6.

FIGURE 6

It is evident that the step model is more effective than the ring model, offering a central fluid velocity that is nearly two times greater. These two models were 3D printed and tested by flowing dyed water through the systems at a rate of 1 mL/day and making observations every 15 minutes. The results from the laboratory tests are seen in Figure 7 which confirm the simulation results. It is apparent that the step bioreactor achieves more drug exposure than the ring bioreactor as evidenced by more dye flowing through the central chamber over the same period of time.

FIGURE 7

4 Discussion

As shown in the previous section, by simply altering the geometry, the flux through the central chamber can be controlled. These findings agree with similar simulations done at the University of Pittsburgh in which a dual fluidic bioreactor was used for high throughput screening [11]. The results indicate that maximization of fluid velocity, and therefore the total drug/nutrients exposure, can be achieved by minimizing the channel diameter and maximizing all other design features. These relationships develop as a result of a rise in the hydraulic resistance of the model. In fact, lengthening the path the fluid has to move through in the surrounding ring or decreasing its channel diameter, the hydraulic resistance is increased and consequently more fluid will move through the central chamber [12]. The sole constraints then are determined by the resolution of the 3D printer and by the overall design considerations of the model.

The step height can be extended only a certain amount before it runs into other portions of the model; therefore, the maximum size for the step height is 1.75 mm. In order to eventually be used in a 96-well plate, the entire ring of the design must fit within a 6.8 mm cylinder. The pore diameter can only be as large as the channel diameter, and, because the channel diameter relationship is logarithmic versus the linear pore diameter relationship, it was determined that the model benefits more from a small channel than large pores. To satisfy these requirements, the following dimensions were chosen:

TABLE 1

5 Conclusions

This optimized step bioreactor maximizes the drug exposure to the cells under test while minimizing the dimensions of the model while allowing for optical access within the 3D construct and maintaining dimensions compatible with a standard 96-well plate.

Having confirmed the predictive value of the simulations, in future research different and unique models can be created and tested in ANSYS to account for specific experimental needs in engineering multiphasic constructs or for delivering drug candidates to specific construct locations. For instance, a dual inlet model can be used to engineer bone on one side of the central chamber with cartilage on the other, and to deliver a compound to only one tissue to assess cartilage-bone interaction, while simultaneously accounting for the possible difference in densities between the two components of the OC construct. Some of these activities are currently being pursued in the laboratory. Furthermore, based on these studies with a single chamber, a bioreactor

comprised of an array of identical units is currently being implemented to allow for medium to

high throughput screening.

6 Acknowledgements

7 References

[1] Lozito T.P., Alexander P.G., Lin H, Gottardi R, Cheng A, Tuan R.S. (2013) *Stem Cell Research & Therapy* 4(Suppl 1):S6.
[2] Goldring S.R., Goldring M.B. (2016) *Nature Reviews Rheumatology* 12:632-44.
[3] Sutherland M.L., Fabre K.M., Tagle D.A., (2013) *Stem Cell Research & Therapy* 4(Suppl 1):I1
[4] Wikswo J.P. (2014) *Experimental Biology and Medicine* 239(9):1061-72.
[5] Iannetti L, D'Urso G, Conoscenti G, Cutrì E, Tuan RS, Raimondi MT, Gottardi R, Zunino P. (2016) *PLoS ONE* 11(9): e0162774.
[6] Lin H., Lozito T.P., Alexander P.G., Gottardi R., Taun R.S. (2014) *Molecular Pharmaceutics* 11(7):2203-12
[7] Taffetani M, Gottardi R, Gastaldi D, Raiteri R, Vena P. (2014) *Medical Engineering and Physics* 36(7):850–8.
[8]http://www.3dsystems.com/products/datafiles/viper/datasheets/International/viper_si2_uk.qxd.pdf
[9] http://www.dsm.com/products/somos/en_US/products/offerings-somos-water-shed.html
[10] http://www.shop.kiyatec.com/Multi-syringe-Pump-Infuse-Withdraw-FC230.htm
[11] G. Conoscenti, G. D'Urso, L. Iannetti, V. La Carrubba, V. Brucato, R.S. Tuan, P. Zunino, R. Gottardi. *Lab on a Chip*. Submitted.
[12] Hsu Y., Moya M., Hughes C., George S., Lee A. (2013) *Lab on a Chip.* 10.1039/c3lc50424g

8 Tables

Table 1: Chosen dimensions for the optimized model

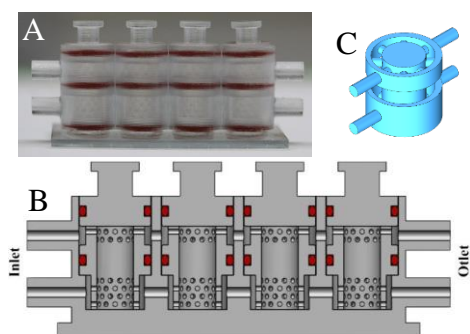| Feature	Dimension
Channel Diameter	0.60 mm
Step Height	1.75 mm
Outer Ring Diameter	6.75 mm
Pore Diameter	0.60 mm
Number of Pores	12

9 Figures

Figure 1: A) Osteochondral bioreactor system (4 wells), B) its cross section, and C) "negative" of one well of the bioreactor highlighting the volume occupied by fluid and constructs.
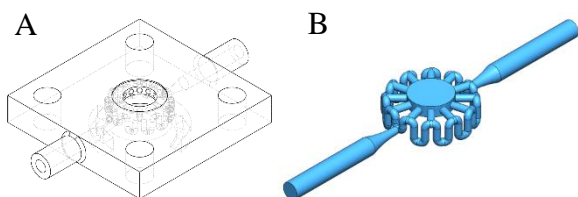

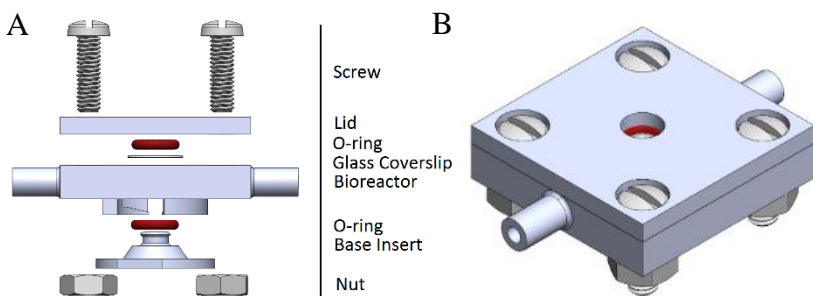**Figure 2:** A) The physical bioreactor, B) volume occupied by fluid and constructs

Figure 3: A) Exploded view of the bioreactor, B) assembled bioreactor model

Location	Feature
A	Channel Diameter
B	Step Height
C	Outer Ring Diameter
D	Pore Diameter
E	Number of Pores

Figure 4: Defining the features of the bioreactor
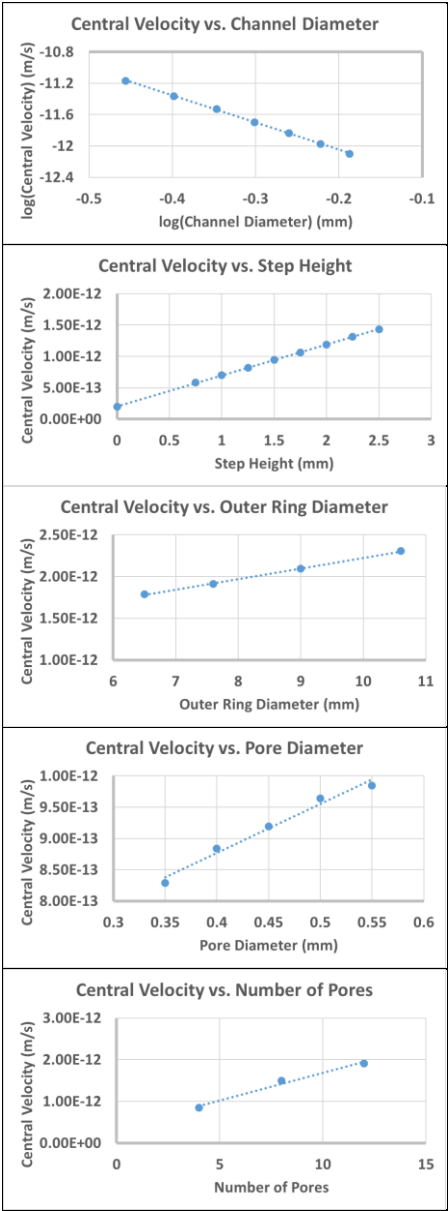
Figure 5: Plots of the central velocity versus various dimensions

	Simple Ring	Optimized Step
Streamlines		
Central Velocity (m/s)	5.026e-13	1.409e-12
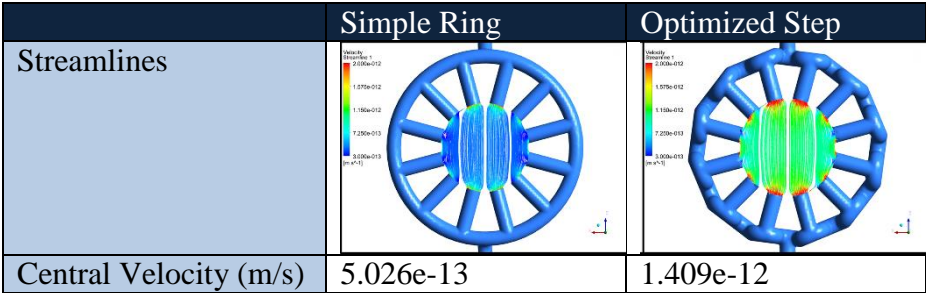
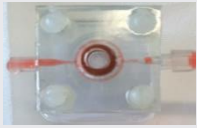**Figure 6:** ANSYS results comparing the simple ring model to the optimized step model

Time (min)	Ring Model	Step Model
15		
30		
45		
60		

Figure 7: Results from laboratory testing proving that the step model attains more drug exposure through the central chamber